2019 International Conference on Robotics and Automation (ICRA)
Palais des congres de Montreal, Montreal, Canada, May 20-24, 2019

Admittance Control for Human-Robot Interaction Using an Industrial Robot Equipped with a F/T Sensor

Eleonora Mariotti Emanuele Magrini Alessandro De Luca

Abstract— **We present an approach to safe physical Human-Robot Interaction (pHRI) for industrial robots, including collision detection, distinguishing accidental from intentional contacts, and achieving collaborative tasks. Typical industrial robots have a closed control architecture that accepts only velocity/position reference inputs, there are no joint torque sensors, and little or no information is available to the user on robot dynamics and on low-level joint controllers. Nonetheless, taking also advantage of the presence of a Force/Torque (F/T) sensor at the end-effector, a safe pHRI strategy based on kinematic information, on measurements from joint encoders and motor currents, and on end-effector forces/torques can be realized. An admittance control law has been implemented for collaboration in manual guidance mode, with whole-body collision detection in place both when the robot is in autonomous operation and when is simultaneously collaborating with a human. Several pHRI experiments validate the approach on a KUKA KR5 Sixx R650 robot equipped with an ATI F/T sensor.**

I. Introduction

Nowadays, robot co-workers are making their way in industrial environments [1], being able to share their workspace with humans, avoiding dangerous situations and collisions, interacting both at the cognitive and physical levels with the operators, and collaborating with them in safe and useful ways. These objectives ask for a combination of novel solutions in the mechanical and actuation design of robots (lightweight/agile arms, compliant joints, variable stiffness actuators) to limit potential injuries for humans, in the use of additional sensory systems to monitor the robot environment, and in the development of intelligent algorithms that control interaction events and signals [2]. With the goal of addressing general issues about physical Human-Robot Interaction (pHRI), we have introduced in [3] a hierarchical control architecture based on three nested layers of desirable robot behaviors, namely safety, coexistence, and collaboration.

Indeed, safety should always be enforced as the primary operative requisite, preventing unintentional human-robot collisions, but also detecting and promptly reacting to them whenever they happen. Robot dependability is increased when such feature can be guaranteed with the minimum use of extra sensors. A successful example of such safety layer is the momentum-based residual method for collision detection and isolation [4], [5], which can be implemented with or without joint torque sensing. However, this method requires a good knowledge of the robot dynamics, a condition that becomes critical when large friction is present and/or for industrial robots whose dynamic model is not made available to end-users. A more rough collision detection can be achieved also by processing just the motor currents [6], [7], but in this case reaction is mainly limited to stopping robot motion without successive interactions.

The control layer that guarantees human-robot coexistence monitors the workspace using external sensors (e.g., vision). Robot motion is then modified online in response to the closeness to humans or other dynamic obstacles. An efficient algorithm for distance computation using depth sensors was presented in [8], while many recent industrial implementations (see, e.g., [9]–[11]) have achieved satisfactory behaviors as well. Standard interfaces and kinematic commands to the robot are in fact already sufficient to the purpose.

As for the collaboration layer, an accurate dynamic model and the possibility of commanding motor currents/torques were shown to be important ingredients for safely controlling the exchange of forces between human and robot. In fact, using again the residual method, contact forces acting anywhere on the robot structure can be estimated [12] and, based on these, a generalized impedance control (with natural or desired inertia) can be realized at the contact point [13]. Moreover, one can also distinguish between intentional (soft) contacts and accidental (hard) collisions, by suitably low-pass filtering the components of the residual vector with different (respectively, small and large) bandwidths, as similarly done also in [14]. These results were obtained on lightweight, compliant robots with an open control architecture that allows to impose motor torques (viz. currents, as their proxy), and after having identified an accurate and complete dynamic model (see, e.g., [15] for the KUKA LWR IV+ and [16] for the Universal Robots UR10). A natural question is whether these results could be transferred to more conventional industrial arms, whose closed architecture provides no access to the user other than via kinematic reference commands, and where a limited knowledge about system dynamics and low-level robot controllers is available.

In our previous work [17], we have shown that collisions of a KUKA KR5 industrial robot with a human user could be detected by processing the motor currents. Moreover, by using low-pass and high-pass filters, one could classify contacts at reasonably low speeds as hard (collision) or soft (intentional). In the latter case, the robot would switch to a collaboration mode, implementing compliant-like behaviors in response to the forces applied by the human operator. The control strategies did not use an explicit measure of the

The authors are with the Dipartimento di Ingegneria Informatica, Automatica e Gestionale, Sapienza Università di Roma, Via Ariosto 25, 00185 Roma, Italy (elemariotti@hotmail.it, {magrini,deluca}@diag.uniroma1.it). This work is supported by the European Commission, within the H2020 projects ICT-645097 COMANOID (comanoid.cnrs.fr) and FoF-637080 SYMPLEXITY (www.symplexity.eu).

contact forces, relying instead only on robot proprioceptive information (joint position and motor currents) and kinematics. In a test campaign with multiple users, we verified that the collaborative behavior obtained when pushing/pulling the robot end-effector was not felt as transparent as expected in response to the (unmeasured) applied forces.

In this paper, we build upon our results in [17] and propose novel interaction strategies for the same class of industrial robots, exploiting the additional presence of a 6D Force/Torque (F/T) sensor mounted on the end-effector. Thanks to the feedback of the measured forces, admittance control laws are designed to handle human-robot interaction and collaboration. Collision detection is performed by filtering either the motor currents or the forces measured by the sensor. In this way, we can better distinguish hard collisions from soft contacts at the end-effector level, and start in the latter case a collaboration by manual guidance in a very effective and natural way for the operator. In addition, we can detect a collision on the robot body even during a human collaboration with the robot end-effector. For this, a signal-based method using motor torque differences is implemented.

The paper is organized as follows. The main characteristics of the industrial robot (with F/T sensor) used in our study are summarized in Sec. II. Section III presents the proposed schemes for safe pHRI, including the kinematic control laws for normal task execution, the detection of collisions, their analysis and handling, and the admittance control laws used for collaboration. Section IV reports on the experiments with a KUKA KR5 (shown in the accompanying video), while the main results are summarized in the concluding Sec. V.

II. KUKA KR5 Robot with ATI F/T Sensor

We considered as target system the KUKA robot KR5 Sixx R650, a small-size serial manipulator with $n = 6$ revolute joints, including a spherical wrist. Figure 1 shows the frames and the associated table of Denavit-Hartenberg (DH) parameters used for kinematic computations. This industrial robot has a typical closed control architecture: the user specifies a six-dimensional joint velocity vector $\dot{\boldsymbol{q}}_r$ (and/or a joint position) as reference input, while having access to the joint position $\boldsymbol{q}$, measured by six encoders, and to the absolute values of motor currents $\boldsymbol{i}$ —see Fig. 2. These input/output signals are exchanged with a user-defined control program every $T_c = 12$ ms ($f_c = 83.3$ Hz), the maximum (but still relatively slow) sampling frequency that can be specified by the KUKA RobotSensorInterface (RSI) [18]. Neither the inner structure of the control blocks local to each motor/joint, nor information on the robot dynamic model are made available by the robot manufacturer.

We shall consider mainly trajectories defined in terms of the end-effector position $\boldsymbol{p} \in \mathbb{R}^3$, whose direct kinematics is

$$\boldsymbol{p} = \boldsymbol{k}_p(\boldsymbol{q}) \tag{1}$$

For the differential kinematics, we use the geometric 6×6

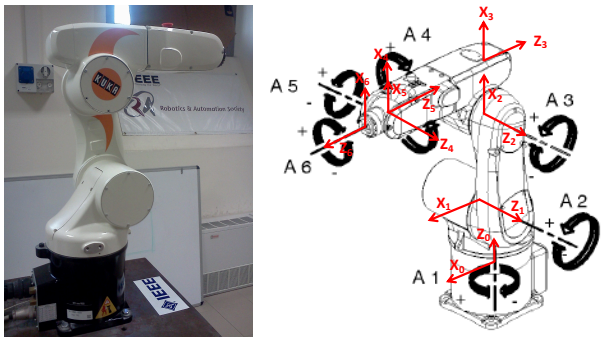

i	α_i	d_i	a_i	θ_i
1	-π/2	$d_1 = 0.132$	$a_1 = 0.075$	$q_1 = 0$
2	0	0	$a_2 = 0.270$	$q_2 = -\pi/2$
3	π/2	0	$a_3 = 0.09$	$q_3 = 0$
4	-π/2	$d_4 = -0.295$	0	$q_4 = 0$
5	π/2	0	0	$q_5 = 0$
6	π	$d_6 = -0.08$	0	$q_6 = 0$

Fig. 1. The KUKA KR5 Sixx R650, with the used Denavit-Hartenberg frames and table of parameters.

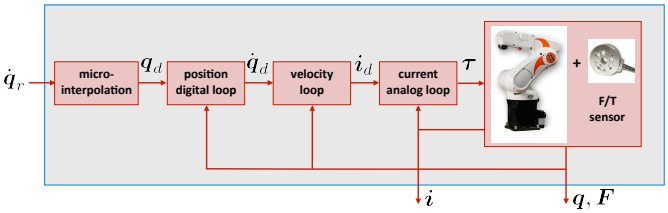

Fig. 2. The closed control architecture of the KUKA KR5 robot equipped with a F/T sensor, with the input and output signals available to the user.

Jacobian matrix $\boldsymbol{J}$ [19]

$$\begin{pmatrix} \boldsymbol{v} \\ \boldsymbol{\omega} \end{pmatrix} = \boldsymbol{J}(\boldsymbol{q})\dot{\boldsymbol{q}} = \sum_{i=1}^{6} \boldsymbol{J}_i(\boldsymbol{q})\dot{q}_i, \tag{2}$$

where $\boldsymbol{J}_i \in \mathbb{R}^6$ is the generic ith column of $\boldsymbol{J}$ and the Jacobian is partitioned as

$$\boldsymbol{J}(\boldsymbol{q}) = \begin{pmatrix} \boldsymbol{J}_p(\boldsymbol{q}) \\ \boldsymbol{J}_o(\boldsymbol{q}) \end{pmatrix}, \qquad \boldsymbol{J}_p(\boldsymbol{q}) = \frac{\partial \boldsymbol{k}_p(\boldsymbol{q})}{\partial \boldsymbol{q}}. \tag{3}$$

The robot is equipped with a 6D Force/Torque (F/T) sensor, the small Mini45 model by ATI Industrial Automation, that is used for measuring contact forces $\boldsymbol{f} \in \mathbb{R}^3$ and moments $\boldsymbol{m} \in \mathbb{R}^3$ at the end-effector, expressed in a frame related to the last DH frame (attached to the robot link 6). We denote collectively these measured quantities as

$$\boldsymbol{F} = \begin{pmatrix} \boldsymbol{f} \\ \boldsymbol{m} \end{pmatrix} \in \mathbb{R}^6, \quad \boldsymbol{f} = \begin{pmatrix} {}^6f_x \\ {}^6f_y \\ {}^6f_z \end{pmatrix}, \quad \boldsymbol{m} = \begin{pmatrix} {}^6m_x \\ {}^6m_y \\ {}^6m_z \end{pmatrix}. \tag{4}$$

The device transmits only analog signals through a screened cable which are acquired and converted at 1 kHz by a Data Acquisition (DAQ) card and its software running on the user computer. These data are elaborated within the user-defined control law, whose output is interfaced via the RSI to the low-level controllers of the KUKA robot.

As noted in [17], only the absolute values of the motor currents (i.e., $|i_j| \geq 0$, rather than i_j for motor j) are available via the RSI interface. This represents a specific limitation of this industrial robot for many of the desirable user-defined control actions, such as gravity compensation by means of a motor current feedforward. In addition, computing differences between absolute values of motor currents may be misleading. In static conditions, we can attribute a sign to each component of the measured motor current vector based on the dominant role of gravity and on a preliminary analysis made on the whole configuration space. However, this is no longer easy to do when the manipulator is in motion. If we know nothing about the robot dynamic model, it is hard to attribute reliably a sign to the motor currents provided by the RSI, and thus to interpret correctly the presence or absence of sudden changes in contiguous time instants. Therefore, wherever possible, we will follow a different strategy in the next section.

III. Safe pHRI

The general algorithm for a safe pHRI works in sequential steps. At every sampling instant, we check if there is a collision on the robot body or a contact/collision on its end-effector. When no collisions nor intentional contacts are being detected, the robot starts/proceeds with the execution of the original motion task. Different types of filters (and thresholds) will be used in the various cases. A first high-pass filter is for whole-body collision detection, and uses a variable thresholding on the absolute values of the motor currents, as first developed in [17]. A second high-pass filter is on the forces measured by the F/T sensor, which monitors possible collisions at the robot end-effector level. When such collisions are detected, the robot stops its motion. In the absence of collisions, the human can request the start of a collaboration phase by pushing softly on the robot end-effector. This situation is recognized by using a third, low-pass filter of the measured forces. We consider also the mixed situation in which the robot body collides against an obstacle/human in the environment, while collaboration is taking place at the end-effector level. In this case, we take advantage of the equivalent motor currents associated to the quantities measured by the F/T sensor (which are known in sign). An admittance control law designed in the Cartesian- or in the joint-space is applied in response to a physical request of collaboration.

A. Kinematic control for normal task execution

During normal operation, a desired Cartesian trajectory $\boldsymbol{p}_d(t) \in \mathbb{R}^3$ is assigned to the end-effector position. The task is thus of dimension $m = 3$. Since there are $n = 6$ joints and $n > m$, the robot will be redundant for this task and an extra control should be exerted on the robot self-motions in the joint space. We use the kinematic control law

$$\begin{aligned} \dot{\boldsymbol{q}}_r &= \boldsymbol{J}_p^{\#}(\boldsymbol{q})\dot{\boldsymbol{p}}_e + \left(\boldsymbol{I} - \boldsymbol{J}_p^{\#}(\boldsymbol{q})\boldsymbol{J}_p(\boldsymbol{q})\right)\dot{\boldsymbol{q}}_0 \\ &= \dot{\boldsymbol{q}}_0 + \boldsymbol{J}_p^{\#}(\boldsymbol{q})\left(\dot{\boldsymbol{p}}_e - \boldsymbol{J}_p(\boldsymbol{q})\dot{\boldsymbol{q}}_0\right), \end{aligned} \tag{5}$$

where

$$\dot{\boldsymbol{p}}_e = \dot{\boldsymbol{p}}_d + \boldsymbol{K}\left(\boldsymbol{p}_d - \boldsymbol{k}_p(\boldsymbol{q})\right), \tag{6}$$

with control gain matrix $\boldsymbol{K} > 0$ (typically, diagonal) on the task error $\boldsymbol{e}_p = \boldsymbol{p}_d - \boldsymbol{k}(\boldsymbol{q})$. Matrix $\boldsymbol{J}_p^{\#}$ is the 6×3 pseudoinverse of the positional task Jacobian $\boldsymbol{J}_p$, the 6×6 matrix $\boldsymbol{I} - \boldsymbol{J}_p^{\#}\boldsymbol{J}_p$ is an orthogonal projector in its null space, and the joint velocity $\dot{\boldsymbol{q}}_0$ helps in shaping the behavior of the robot configuration. The second expression in (5) illustrates the efficient implementation of the control law.

B. Collision detection

Undesired (hard) collisions are represented by measured force or motor current signals with a high-frequency spectrum content. Digital filtering of signals will be followed by a comparison with a (constant or time-varying) threshold that defines the change of interaction state. In the following, denote by $\boldsymbol{y}_k = \boldsymbol{y}(t_k)$ a generic vector signal at time $t = t_k = kT_c$, with components sampled every T_c seconds. Denote by $y_{k,j}$ the jth component of this vector. We will distinguish two situations of collision.

1) Collision with the robot body: This collision is handled according to the filtering process of motor currents $\boldsymbol{i}$. The processing is limited to the first three large joints, certainly the most stressed by gravity and the possible collisions on the robot body. The motor currents are filtered using a digital high-pass Chebyshev filter of order 3,

$$\boldsymbol{i}_{HPF,k} = h_0\boldsymbol{i}_k + h_1\boldsymbol{i}_{k-1} + h_2\boldsymbol{i}_{k-2} + h_3\boldsymbol{i}_{k-3}, \tag{7}$$

with $h_0 = -0.239207$, $h_1 = -0.6262528$, $h_2 = 0.6262528$, and $h_3 = 0.2392073$. This choice corresponds to a cut-off frequency $f_{co} = 10$ Hz.

The filtered motor currents are then compared to time-varying thresholds $\tau_{\mathrm{HPF}}(t)$, depending on the reference (commanded) joint velocities $\dot{\boldsymbol{q}}_r$ and related accelerations $\ddot{\boldsymbol{q}}_r$ (obtained by backward numerical differentiation), as proposed in [17]. For the high-pass filtered motor current, we use

$$\tau_{\mathrm{HPF}} = \tau_{H_{min}} + k_{H_v}\frac{|\dot{q}_r|}{v_{max}} + k_{H_a}\frac{|\ddot{q}_r|}{a_{max}} > 0, \tag{8}$$

with the numerical parameters given in Tab. I. This type of thresholds were implemented in order to avoid false alarms due to large but normal absolute values of currents.

We have also considered collisions that can be followed by an extended period of continuous contact, e.g., when a human is possibly clamped by the robot. While the first few instants of the hard collision will be identified by a peak in the high-pass filter signal, the permanent contact with a uniform applied force can be considered as a soft interaction. Therefore, it is useful to compute also a low-pass filtered version of the motor currents. This was chosen as the simple average of the last three consecutive samples,

$$\boldsymbol{i}_{LPF,k} = \frac{1}{3}\left(\boldsymbol{i}_k + \boldsymbol{i}_{k-1} + \boldsymbol{i}_{k-2}\right). \tag{9}$$

Similar to (8), also the low-pass filtered motor currents are compared to a time-varying threshold,

$$\tau_{\text{LPF}} = \tau_{L_{min}} + k_{L_v} \frac{|\dot{q}_r|}{v_{max}} + k_{L_a} \frac{|\ddot{q}_r|}{a_{max}} > 0, \qquad (10)$$

whose numerical parameters are given again in Tab. I. For more details about filters and thresholds, see [17] and [20]. Parameters were tuned by trials in nominal conditions for maximum dynamic sensitivity while avoiding false positives.

TABLE I

PARAMETERS OF THRESHOLDS ON FILTERED MOTOR CURRENTS

joint		1	2	3
HPF	$\tau_{H_{min}}$	0.1	0.18	0.16
	k_{H_v}	0.1	0.35	0.25
	k_{H_a}	0.2	0.2	0.2
LPF	$\tau_{L_{min}}$	0.1	0.96	0.99
	k_{L_v}	1.6	1.3	1.3
	k_{L_a}	0	0	0
for both HPF and LPF	v_{max}	200	125	100
	a_{max}	1200	1050	900

2) Collision on the robot end-effector: To identify this type of collisions, we use a high-pass filter on the measured forces of the form

$$\boldsymbol{f}_{HPF,k} = \boldsymbol{f}_{HPF,k-1} + \left(\boldsymbol{f}_k - \boldsymbol{f}_{k-1}\right) \alpha_{HPF}, \qquad (11)$$

choosing as cut-off frequency

$$f_{co} = 15 \text{ Hz} \quad \Rightarrow \quad \alpha_{HPF} \simeq 0.5307. \qquad (12)$$

When $\|\boldsymbol{f}_{HPF,k}\| > \varepsilon_{f_{HPF}}$, such a collision is identified. The joint velocity command becomes $\dot{\boldsymbol{q}}_r = \boldsymbol{0}$ and is kept to zero until the undesired contact has been removed. For this to be decided, similar to the previous case of extended contact, we need a low-pass filter for soft interaction. However, since we are now working with measured forces, we will use the filter (13) of the next section III-C on collaboration. When both filtering processes will no longer reveal the presence of a contact, the robot will resume execution of the original task (after a short while, for security reasons).

C. Collaboration

We need to distinguish a hard collision on the robot end-effector from a soft contact, which is assumed to be associated to the human intention to collaborate. Soft contacts are characterized by the absence of high-frequency content in the force signal $\boldsymbol{f} \in \mathbb{R}^3$. Therefore, they will be isolated by low-pass filtering the measured forces. For this, we used a simple first-order digital filter (of the RC type),

$$\boldsymbol{f}_{LPF,k} = \boldsymbol{f}_{LPF,k-1} + \left(\boldsymbol{f}_k - \boldsymbol{f}_{LPF,k-1}\right) \alpha_{LPF}. \qquad (13)$$

The scalar smoothing factor $\alpha_{LPF} \in (0, 1]$ is related to the desired cut-off frequency $f_{co} > 0$ (in Hz) of the filter, as given by

$$\alpha_{LPF} = \frac{T_c}{T_c + T_{co}}, \quad \text{with } T_{co} = \frac{1}{2\pi f_{co}}. \qquad (14)$$

Since the KUKA RSI imposes $T_c = 12$ ms, for the low-pass filter (13) we have set

$$f_{co} = 5 \text{ Hz} \quad \Rightarrow \quad \alpha_{LPF} \simeq 0.2738. \qquad (15)$$

The intentional contact is recognized if $\|\boldsymbol{f}_{LPF,k}\| > \varepsilon_{f_{LPF}}$.

1) Collision during collaboration: Even if the robot is compliant while being manually guided by the human during a collaboration phase, for safety reasons it is necessary to stop its motion whenever a collision (or another undesired contact) is detected on the robot body. To understand if such a collision occurs, we do not use in this case a filtering process, neither on the currents nor on the measured forces.

We first note the following. During collaboration, the absolute value of the jth component of the motor current vector (for $j = 1, \ldots, 6$) at $t = t_k$ can be written as

$$|i_{k,j}| = \left| i_{k-1,j} + \left(\boldsymbol{J}_j^T(\boldsymbol{q}_k)\boldsymbol{F}_k\right)/k_{m,j} \right|, \qquad (16)$$

where $k_{m,j} > 0$ is the current-to-torque drive gain of motor j and we used the notation introduced in (2). The vector $\boldsymbol{i}_{k-1} \in \mathbb{R}^6$ of motor currents, without the contribution of the interaction force at the end-effector level, represents approximately the command used for compensating gravity and executing the nominally planned motion task with the robot. The second term on the right-hand side of (16) represents instead the motor current (i.e., a torque divided by the motor drive gain) that arise from the manual guidance of the robot end-effector. When a collision occurs on the robot body, the motor currents will change and the relation (16) must be rewritten as

$$|i_{k,j}| = \left| i_{k-1,j} + \left(\boldsymbol{J}_j^T(\boldsymbol{q}_k)\boldsymbol{F}_k\right)/k_{m,j} + i_{coll,j} \right|, \qquad (17)$$

where $i_{coll,j}$ is the contribution of the collision on the robot body to the total current of motor j. When measuring motor currents through the RSI interface in our target KUKA KR5 robot, unfortunately we only get positive values. Thus, the subtraction of (16) from (17) will provide no reliable information about $i_{coll,j}$.

We propose to use a different algorithm, which implements a residual-like method that identifies possible collisions on the robot body, based on an estimate of joint torques differences. For $j = 1, \ldots, 6$, define the jth component of the residual vector $\boldsymbol{r}_k = \boldsymbol{r}(t_k)$ as

$$r_{k,j} = |k_{m,j}\,(i_{k,j} - i_{off,j})| - \left| \boldsymbol{J}_j^T(\boldsymbol{q}_k)\boldsymbol{F}_k \right|. \qquad (18)$$

In [17], $i_{off,j}$ was evaluated as the motor current at joint j due to the gravity contribution (in the absence of collaboration). However, when the robot is in dynamic motion and/or in the presence of end-effector force/torque $\boldsymbol{F} \neq \boldsymbol{0}$, this evaluation may lead to critical situations (false positives/negatives). Therefore, we have simply set $\boldsymbol{i}_{off}$ equal to the last measure of motor currents before the start of a collaboration task, canceling this from the actually measured motor currents $\boldsymbol{i}_k$. When there is only the intentional contact at the end-effector, the value of the series of residuals (18) is always about zero. When a collision occurs on the robot body, one or more of the components (18) of the residual vector $\boldsymbol{r}_k$, taken in absolute value, will become larger than a small positive threshold $\varepsilon_r > 0$. Robot motion is then stopped, having recognized the simultaneous presence of an intentional collaboration force and a collision force.

2) Admittance control during collaboration: Once an intentional contact has been isolated, a Cartesian admittance control law is used here to handle the exchanged forces between human and robot. The velocity command $\dot{\boldsymbol{q}}_r$ to the robot is generated kinematically from the end-effector admittance velocity $\boldsymbol{v} \in \mathbb{R}^3$ in response to a Cartesian force, which is composed in turn by the measured force $\boldsymbol{f}$ and by a control action proportional to the position error $\boldsymbol{e} \in \mathbb{R}^3$ w.r.t. the initial position where physical interaction started. The control law is then

$$\dot{\boldsymbol{q}}_r = \boldsymbol{J}_p^{\#} \boldsymbol{v}, \quad \boldsymbol{v} = \boldsymbol{C}_{cart} \boldsymbol{f}_{cart}, \quad \boldsymbol{f}_{cart} = \boldsymbol{f} + \boldsymbol{K}_{P,cart}\, \boldsymbol{e}, \tag{19}$$

with a Cartesian compliance matrix $\boldsymbol{C}_{cart} > 0$, and where the 'equivalent spring' stiffness matrix $\boldsymbol{K}_{P,cart} > 0$ (typically diagonal) is tuned so as to obtain a gentle robot behavior when the human is pushing or releasing contact.

By using (19), the robot becomes compliant at will to the forces applied by the human so that the end-effector can be manually guided around with relative ease. When contact is gone, the robot senses no more forces and will return to the position assumed at the start of interaction with a desired, soft transient. After some time (we arbitrarily set 4 s in the experiments), the robot will resume execution of the original task from the reached position.

IV. Experiments

In order to evaluate the effectiveness of the proposed framework for safe pHRI, with parallel collision detection/reaction and collaboration capabilities, we performed several experiments on a KUKA KR5 Sixx R650 industrial robot, equipped with an ATI Mini45 F/T sensor. The original task was to move cyclically the robot end-effector along a cyclic, piecewise linear path passing through four Cartesian points with rest-to-rest timing profiles. During normal operation, the kinematic control law (5) was used with

$$\dot{\boldsymbol{q}}_0 = \boldsymbol{K}_0(\boldsymbol{q}_d - \boldsymbol{q}), \qquad \boldsymbol{K}_0 = k_0 \boldsymbol{I} > 0, \tag{20}$$

where $\boldsymbol{q}_d = \boldsymbol{q}(t=0)$ is the configuration of the robot when a contact is being detected (resetting then time to $t = 0$), and with a scalar gain $k_0 = 2$. In order to test the detection and reaction to collisions, we consider different situations of possible undesired contacts.

In the first part of the experiment (shown in the accompanying clip), the human operator touches softly the robot end-effector to engage a collaboration phase, as shown in Fig. 3. The intentional contact is recognized by the low-pass filter with threshold $\varepsilon_{f_{LPF}} = 7$ N, as shown in the left side of Fig. 4. Hence, the robot starts the collaboration becoming compliant under the effect of the control law (19), where we chose a compliance matrix $\boldsymbol{C}_{cart} = 0.008 \cdot \boldsymbol{I}$ and a proportional error gain $\boldsymbol{K}_{P,cart} = 300 \cdot \boldsymbol{I}$. As shown on the right of Fig. 4, the high-pass filtered forces do not exceed the threshold $\varepsilon_{f_{HPF}} = 10$ N, since these interaction forces are characterized by low frequencies components (soft contact).

In the second part of the experiment, the human hits in an impulsive way the end-effector, emulating an unexpected

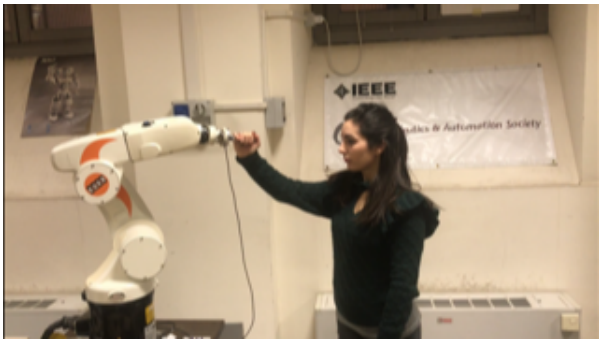

Fig. 3. Robot compliant behavior in a collaborative task: Manual guidance.

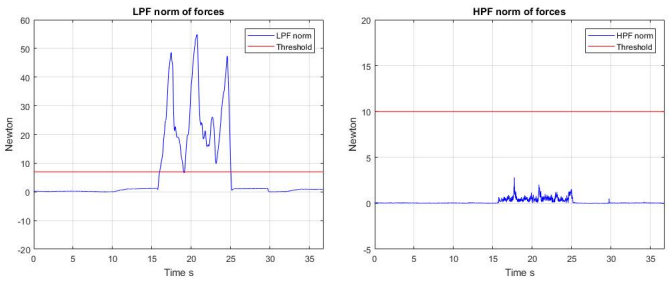

Fig. 4. Norm of low-pass filtered force $\boldsymbol{f}_{LPF}$ (left) and high-pass filtered force $\boldsymbol{f}_{HPF}$ (right) at the end-effector. Collaboration starts at $t \approx 16$ s.

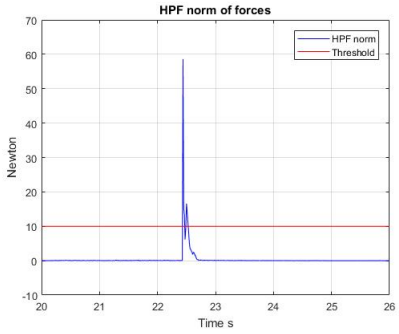

Fig. 5. Norm of the high-pass filtered forces. A collision on the end-effector is detected at $t \approx 22.4$ s.

collision. Thus, the high-pass filter on the measured force is excited and the norm of the filtered forces arises quickly, as shown in Fig. 5. When $\|\boldsymbol{f}_{HPF}\| > \varepsilon_{f_{HPF}}$, collision is detected and the robot stops immediately.

When a collision turns into an extended contact (e.g., the human is clamped by the robot, or obstacles cannot be removed), the robot should be able to recognize the situation. In this case, we use the combination of high-pass and low-pass filtering of forces as in case *2)* of Sec. III-B. With reference to Fig. 6, the high-pass filter is used in order to identify the initial hard impact (at $t \approx 30.4$ s), while the low-pass filter is needed to observe the entire interval of contact. Once this is eventually removed, the robot will resume execution of the original task.

To detect collisions on the robot arm, we evaluated the filtering processes in eqs. (7) and (9), considering the motor currents at the first three joints. The variable thresholds (8) and (10) have been used, with the parameters given in Tab. I.

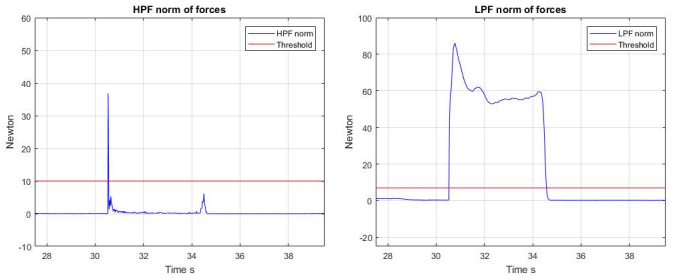

Fig. 6. Norm of the high-pass (left) and the low-pass (right) filtered forces. After the collision is detected at $t \approx 30.4$ s, the contact force is continuously applied at the end-effector for about 4 s.

Similarly to the previous situation, the human hits the robot, now on the 4-th link, emulating an impulsive collision along the robot arm. As shown in Fig. 7, the high-pass filter on the current of the motor at the first joint detects the impulsive collision at $t \approx 46$ s. The low-pass filter is used to understand if the collision is kept for a while. In fact, by combining the signals provided by the high-pass and low-pass filters, a second extended collision (about 3 s long) is detected at $t \approx 58$ s. Due to the geometry of the contact, part of this force is absorbed by the robot structure, so that joint 2 is not able to detect the collision, as shown in Fig. 8 (same behavior for joint 3).

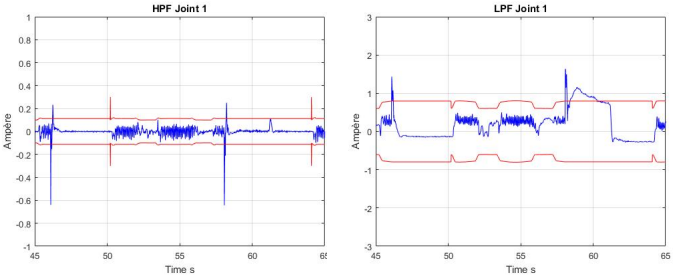

Fig. 7. High-pass (left) and low-pass (right) filtering of motor current at joint 1 with variable threshold.

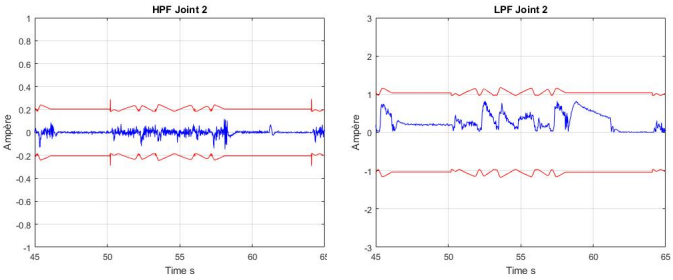

Fig. 8. High-pass (left) and low-pass (right) filtering of motor current at joint 2 with variable threshold.

Finally, we have considered the situation of a collision along the robot arm during a human-robot collaboration. While a first human user interacts with the robot at its end-effector level, a collision with another human occurs along the robot body. This extra collision can be detected through the components of the residual vector defined by (18). When at least one of these exceeds the threshold $\varepsilon_r = 22$ N, collision is detected. Note that, for the residual computations, we consider also the torque provided by the F/T sensor. As shown in Fig. 9, a contact is detected by r_1 at $t \approx 71$ s. The complete experiment can be seen in the accompanying video clip. Plots can be appreciated much better when looking in parallel to the video.

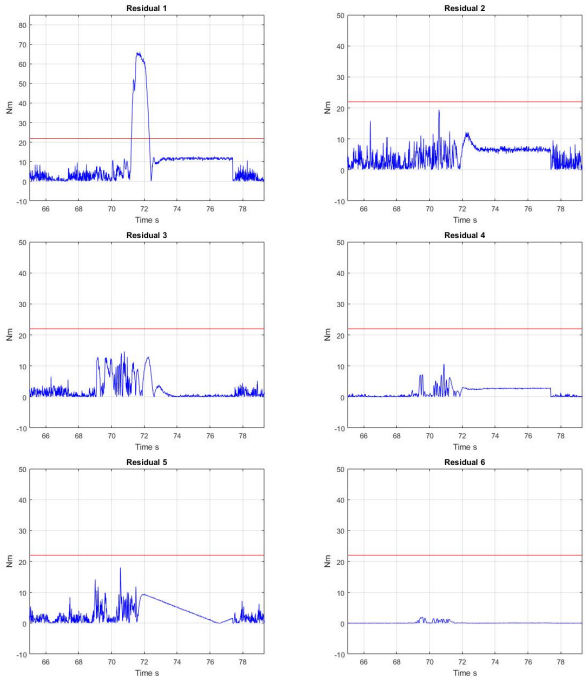

Fig. 9. Components of the motor current residual vector.

V. Conclusions

We have addressed a number of problems that arise in order to guarantee safety and collaboration during pHRI, using a conventional small-size industrial robot in a typical end-user setting with the only additional benefit of a F/T sensor on the end-effector. We moved away from the advantageous situation available in new generations of lightweight and compliant manipulators, considering instead the real-world limitations due to: a closed control architecture that accepts only kinematic commands; no access to information on the robot dynamics and on its joint controllers; lack of joint torque sensing; presence of non-negligible friction; measurement limitations (both in sign and frequency).

Despite these restrictions, we produced a dependable solution that detects collisions on the whole robot body, distinguishing also soft intentional contacts from accidental collisions, and that simultaneously enables natural collaborative behaviors, e.g., manual guidance of an end-effector tool. The proposed controller uses a range of techniques, including low-pass and high-pass filtering of contact forces measured by the F/T sensor and of motor currents, a residual-like scheme for separating torque/current anomalous contributions due to extra collisions, and a kinematic control law that exploits robot redundancy in executing the original task.

REFERENCES

[1] M. Hägele, K. Nilsson, J. Pires, and R. Bischoff, "Industrial robotics," in *Springer Handbook of Robotics (2nd Ed.)*, B. Siciliano and O. Khatib, Eds. Springer, 2016, pp. 1385–1421.

[2] S. Haddadin and E. Croft, "Physical human-robot interaction," in *Springer Handbook of Robotics (2nd Ed.)*, B. Siciliano and O. Khatib, Eds. Springer, 2016, pp. 1835–1874.

[3] A. De Luca and F. Flacco, "Integrated control for pHRI: Collision avoidance, detection, reaction and collaboration," in *Proc. IEEE Int. Conf. on Biomed. Robotics and Biomechatronics*, 2012, pp. 288–295.

[4] A. De Luca, A. Albu-Schäffer, S. Haddadin, and G. Hirzinger, "Collision detection and safe reaction with the DLR-III lightweight robot arm," in *Proc. IEEE/RSJ Int. Conf. on Intelligent Robots and Systems*, 2006, pp. 1623–1630.

[5] S. Haddadin, A. De Luca, and A. Albu-Schäffer, "Robot collisions: A survey on detection, isolation, and identification," *IEEE Trans. on Robotics*, vol. 33, no. 6, pp. 1292–1312, 2017.

[6] K. Suita, Y. Yamada, N. Tsuchida, K. Imai, H. Ikeda, and N. Sugimoto, "A failure-to-safety 'kyozon' system with simple contact detection and stop capabilities for safe human-autonomous robot coexistence," in *Proc. IEEE Int. Conf. on Robotics and Automation*, 1995, pp. 3089–3096.

[7] C.-N. Cho and J.-B. Song, "Collision detection algorithm robust to model uncertainty," *Int. J. of Control, Automation and Systems*, vol. 11, no. 4, pp. 776–781, 2013.

[8] F. Flacco, T. Kröger, A. De Luca, and O. Khatib, "A depth space approach for evaluating distance to objects – with application to human-robot collision avoidance," *J. of Intelligent & Robotic Systems*, vol. 80, Suppl. 1, pp. 7–22, 2015.

[9] M. Bdiwi, M. Pfeifer, and A. Sterzing, "A new strategy for ensuring human safety during various levels of interaction with industrial robots," *CIRP Annals - Manufacturing Technology*, vol. 66, no. 1, pp. 453–456, 2017.

[10] A. Mohammed, B. Schmidt, and L. Wang, "Active collision avoidance for human–robot collaboration driven by vision sensors," *Int. J. of Computer Integrated Manufacturing*, vol. 30, no. 9, pp. 970–980, 2017.

[11] P. Long, C. Chevallereau, D. Chablat, and A. Girin, "An industrial security system for human-robot coexistence," *Industrial Robot: An International Journal*, vol. 45, no. 2, pp. 220–226, 2018.

[12] E. Magrini, F. Flacco, and A. De Luca, "Estimation of contact forces using a virtual force sensor," in *Proc. IEEE/RSJ Int. Conf. on Intelligent Robots and Systems*, 2014, pp. 2126–2133.

[13] ——, "Control of generalized contact motion and force in physical human-robot interaction," in *Proc. IEEE Int. Conf. on Robotics and Automation*, 2015, pp. 2298–2304.

[14] C.-N. Cho, J.-H. Kim, Y.-L. Kim, J.-B. Song, and J.-H. Kyung, "Collision detection algorithm to distinguish between intended contact and unexpected collision," *Advanced Robotics*, vol. 26, no. 16, pp. 1825–1840, 2012.

[15] C. Gaz, F. Flacco, and A. De Luca, "Identifying the dynamic model used by the KUKA LWR: A reverse engineering approach," in *Proc. IEEE Int. Conf. on Robotics and Automation*, 2014, pp. 1386–1392.

[16] C. Gaz, E. Magrini, and A. De Luca, "A model-based residual approach for human-robot collaboration during manual polishing operations," *Mechatronics*, vol. 55, pp. 234–247, 2018.

[17] M. Geravand, F. Flacco, and A. De Luca, "Human-robot physical interaction and collaboration using an industrial robot with a closed control architecture," in *Proc. IEEE Int. Conf. on Robotics and Automation*, 2013, pp. 4000–4007.

[18] *KUKA.RobotSensorInterface (RSI)*, KUKA System Technology, Augsburg, Germany, 2007, revision 2.

[19] B. Siciliano, L. Sciavicco, L. Villani, and G. Oriolo, *Robotics: Modeling, Planning and Control*, 3rd ed. London: Springer, 2008.

[20] E. Mariotti, "Admittance Control for Human-Robot Interaction Using an Industrial Robot Equipped with a F/T Sensor," Master's thesis, DIAG, Sapienza Università di Roma, January 2018.